Multi-objective MCTLBO approach to allocate renewable energy system (PV/BESS) in electricity grid: assessing grid benefits

Kumari Kasturi and Manas Ranjan Nayak*

Department of Electrical Engineering,
Siksha 'O' Anusandhan University,
Bhubaneswar, Odisha, 751030, India
Email: kumari.kasturi1986@gmail.com
Email: manasnk72@gmail.com
*Corresponding author

Abstract: With the advent of the smart grid paradigm many distribution system operators are making efforts to modernise their power grids through the optimal integration of renewable energy system (RES) such as photovoltaic/battery energy storage system (PV/BESS).This paper presents a novel mathematical model and solution approach for the optimal allocation of RES in radial distribution system (RDS). The optimal allocation of RES is formulated as a problem, and it is solved by multi-objective multi-course teaching learning based optimisation (MCTLBO). An efficient codification for the allocation of RES allows the multi-objective MCTLBO to find the optimal location, capacity and power dispatch of RESs for a given RESs for a given load level with time of use (TOU) pricing. The proposed methodology is tested on the 69-bus RDS. It was found that an appropriate allocation of RESs results techno-economic improvement for the system under study.

Keywords: photovoltaic system; battery energy storage system; BESS; radial distribution system; RDS; MCTLBO.

Reference to this paper should be made as follows: Kasturi, K. and Nayak, M.R. (2020) 'Multi-objective MCTLBO approach to allocate renewable energy system (PV/BESS) in electricity grid: assessing grid benefits', *Int. J. Energy Technology and Policy*, Vol. 16, No. 1, pp.1–23.

Biographical notes: Kumari Kasturi is presently working as an Assistant Professor in the Department of Electrical Engineering, Institute of Technical Education and Research, Siksha 'O' Anusandhan University, Bhubaneswar, Odisha, India. Her research interests are renewable energy, electric vehicles, soft computing and evolutionary computing techniques and its application to power system planning, operation and control.

Manas Ranjan Nayak is presently working as an Associate Professor in the Department of Electrical Engineering, Institute of Technical Education and Research, Siksha 'O' Anusandhan University, Bhubaneswar, Odisha, India. His research interests are renewable energy, electric vehicles, soft computing and evolutionary computing techniques and its application to power system planning, operation and control.

1 Introduction

Integration of renewable sources like solar photovoltaic (PV) into existing distribution network along with storage facility is technically and economically viable, making it an area of intense research. Hybrid power generation systems with renewable sources have been increased at modern context due to its economical and environmental benefits (Omran et al., 2011; Sherwood, 2011).Solar irradiance varies according to the time of the day and different climate conditions (Mohammadi et al., 2014). If PV is allocated close to network loads can lead power loss minimisation, voltage profile and security margin improvement, transmission-distribution upgrade deferral etc. (Khatod et al., 2013). However, intermittent nature of renewable sources with demand variations has introduced many challenges to distribution systems, which may be solved by using battery storage systems (Sugihara et al., 2013). Battery energy storage (BES) systems help in continuous renewable power injection into distribution system, mitigating the power quality issues and maintaining the system constraints (Hill et al., 1996). Therefore, the use of battery energy storage system (BESS) with renewable energy sources such as PV makes the operation more flexible and reliable. In a grid connected PV system with storage, the grid supplies the demand in the case of shortage of power generated at the load end and in the case of surplus generated power, the excess amount is sold back to the utility grid.

Several research works have employed various methods for allocation of grid-connected renewable sources with storage systems. Multi objective index technique was used to optimise size and power factor for hybrid PV and BES system to improve voltage stability and reduce the energy loss (Hung et al., 2014). Multi objective particle swarm optimisation (MOPSO) was introduced to find the size and location of DG along with their type and number (Suchitra et al., 2016). A multi-objective PSO based optimisation tool was used to design DG units in distribution network for reduction of power loss with improved voltage stability (Kayal and Chanda, 2013). The fuzzy decision based multi-objective optimisation technique with a self-adaptive GA was proposed to get appropriate type for sustainable energy considering power loss, voltage offset and operating cost (Shanyi et al., 2016). The benefit of using BES system under time of use (TOU) pricing was based on the optimal battery size (Aksanli and Rosling, 2013). Optimal power allocation is a well studied topic in the literature. It is therefore important to have conducted a thorough literature study to ensure this paper's uniqueness. The proposed energy management strategy (EMS) of RES unit in this paper aims to provide an optimal intra-day power allocating schedule. The objective of this EMS is to minimise the network parameters like active power loss, voltage offset and security margin of an IEEE-69-bus RDS integrated with solar PV systems as well as BES simultaneously by formulating two scenarios each consisting a combination of two objective functions which has not been performed earlier. This will offer both technical and financial incentive to the utility grid to become better aware of the advantages, in terms of both cost and sustainability, that RES units are able to provide.

In order to fulfil the main objective of this work, the scope of the research work is summarised as follows.

- Performance evaluation of distribution network is carried out with load flow constraints consideration such as voltage level and maximum line current capacity limitation after integration of RES units.
- The real time data of solar PV generation and TOU electricity price on a day-basis are considered.
- Introducing a scheduling strategy for the solar PV, BES and the utility grid to minimise the active power loss, voltage offset and security margin by storing low price energy and PV surplus generation to dispatch during peak hour periods.
- Proposing a segment-based performance evaluation strategy to utilise hourly state of charge of the storage in addition to hourly load and PV generation data affected by the weather changes.
- Combining the above mentioned strategies to define the RES unit sizing and placement framework for 69-bus radial distribution system using multi-objective multi-course teaching learning based optimisation (MCTLBO). The results are compared with another optimised method, i.e., multi-objective non-dominated sorting genetic algorithm (NSGA-II).

The rest of the paper is organised as follows. In Section 2, the modelling of the system is described and Section 3 presents the EMS. The problem formulation and the multi-objective MCTLBO are described in Section 4 and Section 5 respectively. The results and discussions are presented in Section 6. Finally, the conclusion is presented in Section 7.

2 Modelling of the system

The system overview of power management for the RES is presented in Figure 1. The RES, utility grid and load were connected to a common AC bus bar. A PV inverter was used to convert the DC output of the PV panel into AC output at the AC bus bar. An inverter/charger unit was used between AC bus and the BESS to convert AC to DC and DC to AC, while charging and discharging the battery respectively. The RESs were connected to the RDS at i^{th} load bus. The 24-h load demand was assumed to follow the IEEE reliability test system load profile (Grigg et al., 1999) and a lagging power factor. The loads and RESs were distributed equally at each phase at load bus. The RESs were assumed to generate active power and reactive power in compliance with the IEEE 1547 standard (IEEE Std., 2003). Gelled electrolyte sealed batteries, which are a type of valve-regulated lead-acid battery, were used because of the requirement of frequent charging and discharging. Backward and forward sweep based algorithm has been used for distribution system load flow analysis (Nayak and Nayak, 2013) due to its high computational efficiency with robust convergence characteristic.

Figure 1 Radial distribution system with RES

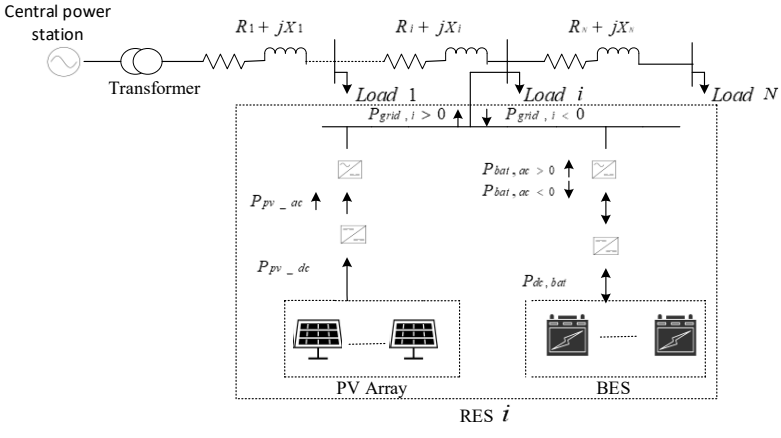

2.1 Modelling of the photovoltaic system

The PV panel output dc power depends on the global horizontal irradiation and the efficiency of the panel at standard temperature condition considering the de-rating due to temperature, manufacturer's output tolerance, dirt, and dc cable loss (Kanzumba, 2015; Ghazvini et al., 2015).

$$P_{pv\_dc}(t) = A_{pv} \times \eta_{pv} \times \eta_{pt} \times I(t) \times N_{pv} \times f_{man} \times f_{dirt} \times f_{cell} \times \eta_{pv\_inv} \tag{1}$$

where is η_{pv} = PV generator reference efficiency = 15%, A_{pv} = area of the PV panel = 33 m^2 (for a PV panel of 5-kW rating), η_{pt} = efficiency of perfect maximum power point tracker = 100%, $I(t)$ = solar insolation at hour t, N_{pv} = number of PV panels, f_{man} = 97% (de-rating factor for manufacture tolerance of 3%), f_{dirt} = 95% (de-rating due to dirt = 5%), $\eta_{pv\text{-}inv}$ = 97% (cable loss between the panel and inverter is 3%).

The de-rating factor due to temperature (f_{cell}) is given by

$$f_{cell} = \left[1 - T_{co} \times \left(T_m - T_{ref}\right)\right] \tag{2}$$

where T_{co} = temperature coefficient = 0.005(varies from 0.004 to 0.006 for silicon cells, the average value is taken), T_{ref} = reference temperature = 25°C (for top-of-pole mount, free standing frame and frame on roof with tilt angle +20 degrees to slope of roof).

The module temperature (T_m) is calculated as follows:

$$T_m = T_{amb} + \left(\frac{NOC - 20}{800}\right) \times I(t) \tag{3}$$

where nominal operating cell temperature (NOC) = 47.6°C (varies from 45.3°C to 49.8°C, the average value is taken), T_{amb} = ambient temperature = 27°C.

The AC output at the AC bus bar is calculated as follows:

$$P_{pv\_ac}(t) = P_{pv\_dc}(t) \times \eta_{inv} \times \eta_{inv\_sb} \tag{4}$$

where η_{inv} = inverter efficiency = 97%, $\eta_{inv\text{-}sb}$ = 99% (AC cable loss ≤ 1% is considered to be associated with the voltage drop between the inverter and primary switch board).

Solar radiation data for Bhubaneswar for the year 2015 was collected from the Indian Meteorological Department. The daily insolation data is as shown in Figure 2.

Figure 2 Average hourly solar insolation and hourly weight factor of load in a day (see online version for colours)

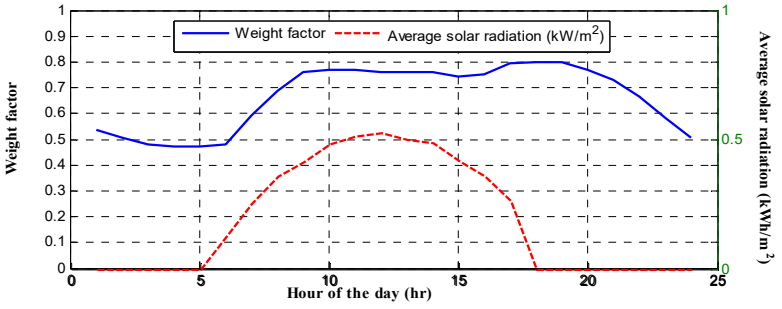

2.2 *Modelling of battery energy storage system*

The status of the BESS system at hour t is related to its status at hour t – 1, the output power of the PV panel, and the load demand at time t (Ton et al., 2008). The variables used for optimising the energy schedule are given and explained in Table 1.

Table 1 Battery specifications

Name of the parameter	*Specification*
Individual BES capacity (Ah)	1,500
Nominal battery voltage (V)	12
Self discharging factor (σ)	2.5% per month
Minimum state of charge (SOC^{min})	30%
Maximum state of charge (SOC^{max})	90%
Minimum charging/discharging time (t_{min})	10 h
Battery round trip efficiency (η_{bat})	81%
Battery charging efficiency ($\eta_{charging}$)	90%
Battery discharging efficiency ($\eta_{discharging}$)	90%

The available capacity of the battery bank at time t can be calculated as follows:

- during peak hours,

$$C_{bat}(t) = \begin{cases} C_{bat}(t-1)(t-\sigma) & SOC(t) \le SOC^{\min} \\ C_{bat}(t-1)(1-\sigma) - \left[\dfrac{P_{load}(t)}{\eta_{inv}} - P_{pv\_ac}(t)\right]\eta_{bat} & SOC(t) > SOC^{\min} \end{cases} \quad (5)$$

- during off-peak hours,

$$C_{bat}(t) = \begin{cases} C_{bat}(t-1)(t-\sigma) & SOC(t) \geq SOC^{\max} \\ C_{bat}(t-1)(1-\sigma) + \left(P_{pv\_ac}(t)\right)\eta_{bat} & SOC(t) < SOC^{\max} \end{cases} \quad (6)$$

where $C_{bat}(t)$ and $C_{bat}(t-1)$ are the capacity of the battery at hour t and $t-1$, respectively, P_{load} = load demand at hour t and η_{bat} = battery round-trip efficiency.

The state of charge (SOC) of the battery is updated every hour with the charging and discharging of power to and from the battery.

Charging,

$$SOC(t) = SOC(t-1)\times(1-\sigma) + \eta_{charging}\frac{P_{dc,bat}(t)}{C_{bat}(t)\times V} \quad (7)$$

Discharging,

$$SOC(t) = SOC(t-1)\times(1-\sigma) + \eta_{discharging}\frac{P_{dc,bat}(t)}{C_{bat}(t)\times V} \quad (8)$$

where $SOC(t)$ and $SOC(t-1)$ are the SOC of the battery at hour t and $t-1$, respectively, V is the nominal battery voltage and $P_{dc,bat}(t)$ is the charging/discharging rate of the battery. $P_{dc,bat}(t)$ is defined by using the equation

$$P_{dc,bat}(t) = E_{bat}(t) - E_{bat}(t-1) \quad (9)$$

where $E_{bat}(t)$ and $E_{bat}(t-1)$ are the stored energy in the battery (kWh) at hour t and $t-1$, respectively.

The AC output at the AC bus bar is calculated as follows:

$$P_{bat,ac}(t) = P_{dc,bat}(t)\times\eta_{inv}\times\eta_{inv\_sb} \quad (10)$$

where η_{inv} = inverter efficiency = 97%, $\eta_{inv\text{-}sb}$ = 99% (AC cable loss accounting for the voltage drop between the inverter and the primary switch board, not more than 1%).

2.3 Modelling of the load

To form a load model, hourly weight factors are used, as shown in Figure 2. The IEEE reliability test system load profile (Grigg et al., 1999) is considered for formulating a 24-hr profile of load weight factors.

The predicted load at bus i at any desired time t can be calculated as follows:

$$P_{Load,i}(t) = w_h(t)\times P_i \quad (11)$$

where $w_h(t)$ = hourly weight factor and P_i = peak load at bus i.

3 Energy management strategy

The operation strategy of the system is classified into two scenarios.

- Scenario-A during off-peak hour of the day: the net PV power will charge the BESS provided that its SOC is less than $SOC^{\max}$. In this case, if the net PV power is less than maximum charging rate of BESS, then battery charges with a rate that is equal to the net generated power. Otherwise, it will charge at its maximum rate. If the BESS is at its $SOC^{\max}$, then the net generated PV power ($P_{surplus}$) will be sold to the grid.

$$P_{grid}(t) = P_{Load,i}(t) - P_{surplus}(t) \tag{12}$$

  If the net PV power is not available, then the BESS is fed by the grid only ($P_{deficit}$). BESS is not allowed to discharge during this period. Because, selling the stored energy to the grid during peak hour gives better economy profitability.

$$P_{grid}(t) = P_{Load,i}(t) + P_{deficit}(t) \tag{13}$$

- Scenario-B during peak hour of the day: The net PV power is sold to the grid as the cost is higher during peak hour. If the SOC of the BESS is greater than $SOC^{\min}$, then BESS also discharges to sell power to the grid. Otherwise the BESS remains idle.

$$P_{grid}(t) = P_{Load,i}(t) - P_{pv,ac}(t) - P_{bat,ac}^{disch}(t) \tag{14}$$

$$P_{grid}(t) = P_{Load,i}(t) - P_{pv,ac}(t) \tag{15}$$

where, p_{grid} is the active power delivering/consuming with the grid.

The reactive power delivering/consuming with the grid can be calculated as follows:

$$Q_{grid}(t) = P_{grid}(t) \times \tan\left(\cos^{-1}(pf)\right) \tag{16}$$

where pf is the power factor of RES.

4 Problem formulation

The proposed RES is integrated into the RDS for reducing power loss, ensuring secure operation and that the voltage levels are within the limit. The total power loss at each hour of each branch in the balanced RDS is obtained from the power flow solution. The proposed multi-objective MCTLBO model is formulated as a multi-objective, multi-period, and nonlinear constrained minimisation problem. One day is divided into 24 h as η_t time slots and the optimisation problem is solved considering the total time slots. The main objective of the proposed method is to determine the optimal allocation for PV and BESS. The problem is solved as a multi-objective, which includes power loss ($f_{obj,1}$), voltage offset ($f_{obj,2}$) and security margin ($f_{obj,3}$) in RDS.

4.1 Objective function

4.1.1 Power loss

$$f_{obj,1} = \frac{1}{n_t} \sum_{t=1}^{n_t} P_{Loss,ij} \tag{17}$$

$$P_{Loss,i}(t) = R_{ij} I_{ij}^2(t) \tag{18}$$

where i = branch number, R_{ij} = resistance of the ij^{th} branch, $I_{ij}(t)$ = current at ij^{th} branch at time t and $P_{Loss,ij}(t)$ = power loss of ij^{th} branch at time t. This modelling improves the energy efficiency.

4.1.2 Voltage offset

$$f_{obj,2} = \frac{1}{n_t}\sum_{t=1}^{n_t}\left(\frac{\sqrt{\sum_{i=1}^{N}\left[\left(\left[\frac{U_i(t)-1}{0.05}\right]\times 10+\left(\frac{|U_i(t)-1|}{0.05}\right)\right)\times 0.05\right]^2}}{N}\right) \tag{19}$$

where $U_i(t)$ = voltage of i^{th} bus at time t and N = number of buses. A voltage range of 90%–110% is permitted for the calculation of voltage offset with a penalty function. The voltage offset is considered as 5%.

4.1.3 Security margin

$$f_{obj,3} = \frac{1}{n_t}\sum_{t=1}^{n_t}\left(1-\min_{ij}\left|\frac{I_{ij}(t)-I_{ij}^r}{I_{ij}^r}\right|\right) \tag{20}$$

where $I_{ij}(t)$ = current at ij^{th} branch at time t and I_{ij}^r = rated current of ij^{th} branch. Under unpredicted loads and discrepancy of microgrid, this modelling provides secure operation.

4.2 System operational constraints

The solution of the optimisation problem considers the following constraints:

$$P_{sub}(t) \pm P_{grid}(t) = P_{Load}(t) + P_{Loss}(t) \tag{21}$$

$$Q_{sub}(t) \pm Q_{grid}(t) = Q_{Load}(t) + Q_{Loss}(t) \tag{22}$$

$$U_i^{\min} \le U_i(t) \le U_i^{\max} \tag{23}$$

$$I_{ij}(t) \le I_{ij}^{\max} \tag{24}$$

$$P_{pv\_dc}^{\min} \le P_{pv\_dc}(t) \le P_{pv\_dc}^{\max} \tag{25}$$

$$P_{dc,bat}^{\min} \le P_{dc,bat}(t) \le P_{dc,bat}^{\max} \tag{26}$$

$$SOC^{\min} \le SOC(t) \le SOC^{\max} \tag{27}$$

where +ve and –ve sign are used for delivering and consuming power with the grid respectively; $P_{sub}(t)$ and $Q_{sub}(t)$ are the active and reactive power injection of substation at time t respectively ; $P_{Load}(t)$ and $Q_{Load}(t)$ are the predicted active and reactive load at time t respectively; $U_i(t)$ is the voltage of bus i; $U_i^{\min}$ and $U_i^{\max}$ are the minimum and maximum voltage of bus i; $I_{ij}^{\max}$ is the maximum current at ij^{th} branch; $P_{pv\_dc}^{\min}$ and $P_{pv\_dc}^{\max}$

are the minimum and maximum dc output power of the PV units, respectively; $P_{dc,bat}^{\min}$ and $P_{dc,bat}^{\max}$ are the minimum and maximum dc output power of the battery, respectively; and $SOC^{\min}$ and $SOC^{\max}$ are the minimum and maximum SOC of the battery, respectively.

5 Multi-objective multi-course teaching learning based optimisation algorithm

5.1 Multi-objective optimisation

The general expression of multi-objective problem is given in equation (28)

$$\begin{aligned} &\min F(x) = \left(f_1(x), f_2(x), ..., f_w(x)\right) \\ &x \in S \\ &x = \left(x_1, x_2, ..., x_n\right) \end{aligned} \tag{28}$$

where $f_1(x)$, $f_2(x)$, …, $f_3(x)$ are the w objective functions, (x_1, x_2, …, x_n) are the n optimisation parameters, and $S \in R^n$ is the solution and parameter space. In multi-objective algorithm, all of the objective functions cannot be optimised simultaneously with one optimal solution. So another approach of Pareto optimal solution is provided. When a minimisation problem and two solution vectors x, $y \in S$ are considered, x is said to dominate y, as denoted $x \succ y$, if

$$\begin{aligned} &\forall i \in 1, 2, ..., k \left| f_i(x) \le f_i(y) \wedge \right. \\ &\exists j \in 1, 2, ..., k \left| f_j(k) < f_j(y) \right. \end{aligned} \tag{29}$$

In a multi-objective optimisation problem, the set of all non-dominated solutions are known as Pareto optimal set. For multi-objective problems, the optimisation aim is to find the entire Pareto-optimal set or its subset.

5.2 Teaching learning based optimisation

The basic teaching learning based optimisation (TLBO) was first suggested by Rao et al. (2011). The meta-heuristic evolutionary algorithm is based on teaching and learning activities in a class room. Two phases of TLBO are teacher phase and learner phase (Rao et al., 2011).

5.3 Multi-course TLBO

There are four phases in MCTLBO to deal with multi-objective problems which are described as follows.

5.3.1 Non-dominated set construction

To create non-dominated set, a removing dominated solution method is used. Identification of first non-dominated front is done in this method. After this method non-dominated sorting technique is applied to sort the solutions. So the proposed algorithm has lower computational complexity. Initially, the non-dominated set size is

assigned to zero, hence considered an empty set. Among the population for each solution $\overline{X}_i$, the following steps are applied: if non-dominated set is an empty set, $\overline{X}_i$ is added into the set. Else $\overline{X}_i$ is compared with each solution $\overline{X}_j$ in the non-dominated set, after comparison if $\overline{X}_i$ dominates $\overline{X}_j$ then $\overline{X}_j$ is deserted and among all the non-dominated solution if $\overline{X}_i$ cannot be dominated by any solution then we add it to the set.

The crowding distance assignment method is applied to find out crowding distance of each solution. It can be assumed that extreme solutions are having largest or smallest function values. Crowding distance calculation for two-objective optimisation problem is shown in Figure 3. The non-dominated solutions are represented as solid dots. Out of five solutions A1 and E1 are extreme solutions among other intermediate solutions. In non-dominated set, let i_{dis} be the crowding distance of any solution. For intermediate solutions, i_{dis} is equal to the addition of absolute differences between two function values of its nearest solutions. That is why i_{dis} of solution C1 is equal to the sum of d1 and d2.

Figure 3 An example of crowding distance calculation

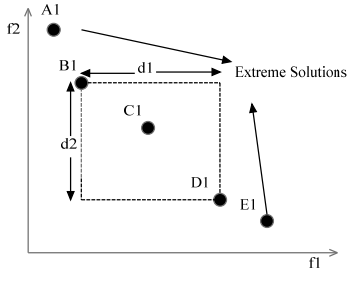

5.3.2 Teacher phase

In general, the basic courses of students in middle school are English, Mathematics, Physics and Chemistry and so on. Each course requires one teacher. Multiple courses are similar to multiple objectives in MOPs, and course scores are similar to objective function values. The solution (i.e., extreme solution) with the best function values of the i^{th} objective is considered as the teachers of the i^{th} course. Besides extreme solutions, solutions with the largest crowding distance among the rest solutions in the non-dominated set are considered as teachers to keep the diversity of population and improve solutions' performance comprehensively. Therefore, the first modification in MCTLBO is achieved by introducing more than one teacher for students. Solutions in a non-dominated set are sorted in descending order of crowding distance. Then, solutions with the largest crowding distance are selected as teachers. Other solutions in the population are improved by those teachers simultaneously in this phase. The basic TLBO is simpler than other evolutionary algorithms as it does not require any algorithm parameters, which are tuned before or during algorithms execution, and their values have significant influences on the algorithm's performances. However, one algorithm parameter, namely teacher count, should be specified in MCTLBO. In basic TLBO algorithm, the teaching factor is either one or two, which indicates that students learn either 0% or 100% from the teacher. But in actual cases students' learning capability are

normally distributed in the range of 0% and 100%. Students may learn any proportion (between zero and one) of the entire things taught by the teacher. The value of teaching factor affects the algorithm's convergence and exploration capability. Quicker convergence and worse exploration capability would result from a larger teaching factor. The teaching factor is calculated as follows:

$$T_F = \frac{M_i}{M_{new}} \tag{30}$$

where Mi is the mean of the class in iteration i, and M_{new} is the current teacher. Thus, the teaching factor automatically adjusts the influence of teachers on students.

$$T_F = \begin{cases} 2 & \text{if } T_F > 2 \\ T_F & \text{if } 1 \le T_F \ge 2 \\ 1 & \text{if } T_F < 1 \end{cases} \tag{31}$$

Thus, the teaching factor automatically adjusts the influence of teachers on student.

5.3.3 Teacher training phase

In the non-dominated set, the rest solutions are considered as candidate trainers. Each teacher T_i improves the performance from a randomly selected trainer. T_i is updated by as follows:

$$T_{new,i} = T_{old,i} + r_i \times (T_{trainer} - T_i) \tag{32}$$

where r_i is a random number in (0, 1). A selection operator is used to choose an solution from $T_{new,i}$ and $T_{old,i}$. If $T_{new,i}$ dominates $T_{old,i}$, $T_{new,i}$ is accepted and $T_{old,i}$ is deserted. If they are not dominated with each other, a coin is flipped to determine which one to be accepted. Figure 4 illustrates the process of selection operator.

Figure 4 The process of selection operator

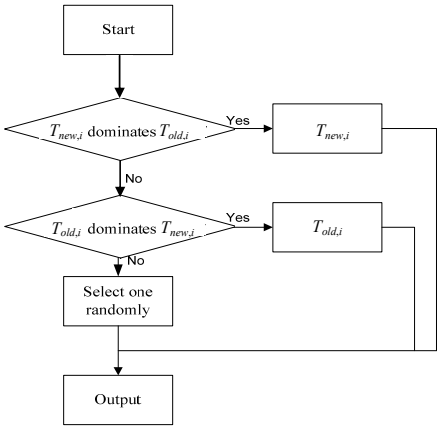

5.3.4 Exchange student phase

A student, who studies at one of his or her school's associate institution, is known as an exchange student. Both the local students and the exchange student coming from another school can improve themselves by mutual interactions. In this phase, a mutation operator introduces an exchange student into the current class. Three different solutions are randomly chosen from the non-dominated set. Let $\bar{X}_1$, $\bar{X}_2$ and $\bar{X}_3$ denote those selected solutions. The mutation process is illustrated as follows.

$$R = \left|f(\bar{X}_1)\right| + \left|f(\bar{X}_2)\right| + \left|f(\bar{X}_3)\right| \tag{33}$$

$$R_1 = \left|\frac{f(\bar{X}_1)}{R}\right| \tag{34}$$

$$R_2 = \left|\frac{f(\bar{X}_2)}{R}\right| \tag{35}$$

$$R_3 = \left|\frac{f(\bar{X}_3)}{R}\right| \tag{36}$$

$$\begin{aligned} X_{exchange} = &\left(\frac{\bar{X}_1 + \bar{X}_2 + \bar{X}_3}{3}\right) + (R_1 - R_2)(\bar{X}_2 - \bar{X}_1) + (R_2 - R_3)(\bar{X}_3 - \bar{X}_2) \\ &+ (R_3 - R_1)(\bar{X}_1 - \bar{X}_3) \end{aligned} \tag{37}$$

where $\left|f(\bar{X})\right|$ is the objective function vector norm. Then, a coin is flipped to determinate whether the exchange student is accepted or not. If so, a student is arbitrarily chosen from the population and abandoned.

5.3.5 Experiment and discussion

A series of simulation experiments have been conducted to examine the performance of MCTLBO. Its results are compared with those that are provided in (Ali and Khan, 2013). The proposed algorithm is compiled in MATLAB 2016R in a personal computer with Windows 10 operation system, a 8th Gen core i5 processor and 8GB RAM. A true Pareto front is a non-dominated set of solutions of a multi-objective problem which is known as the approximate Pareto front. A set of 1001 uniformly spaced Pareto optimal solutions, denoted by is Γ, is chosen from the approximate Pareto front (denoted by $\tilde{\Gamma}$). The following two standard performance criteria are considered to compare the proposed algorithm with the previously discussed algorithms.

Figure 5 The flowchart of MCTLBO algorithm

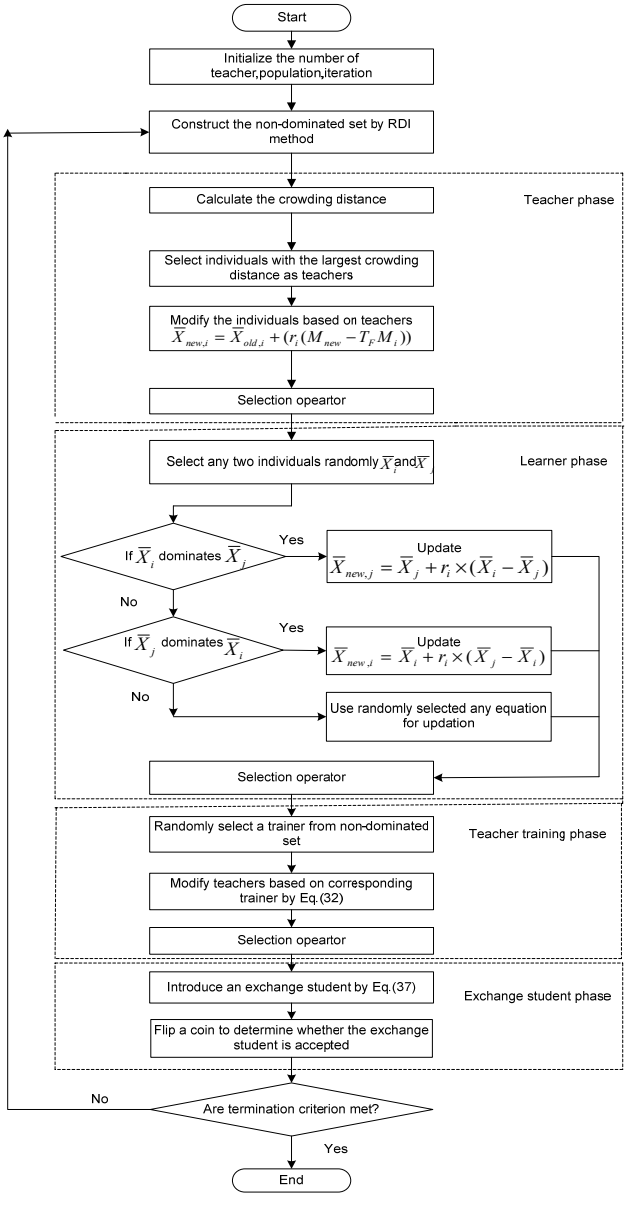

5.3.5.1 Generational distance

Generational distance (Van Veldhuizen, and Lamont, 1998) is a measure of error between Γ and $\tilde{\Gamma}$. It determines the extent of convergence of Γ to $\tilde{\Gamma}$ and is calculated as:

$$GD = \frac{\sum_{i=1}^{|\tilde{\Gamma}|} d_i^2}{|\tilde{\Gamma}|} \tag{38}$$

where $|\tilde{\Gamma}|$ is the number of solutions in $\tilde{\Gamma}$ and d_i is the Euclidean distance of solution i in $\tilde{\Gamma}$ to the nearest pareto-optimal solution Γ. d_i is calculated as:

$$d_i = \min_{j=1}^{|\Gamma|} \left| f_i - f_j \right| \tag{39}$$

where $|\Gamma|$ is the no. of solutions in Γ, f_i is the objective function value vector of solution i in $\tilde{\Gamma}$ and f_j is the objective function value vector of solution j in Γ. Lower value of GD ensures that the $\tilde{\Gamma}$ has a lower approximation error.

5.3.5.2 Diversity metric

Diversity metric (Deb et al., 2002) is a measure of the extent of the spread in $\tilde{\Gamma}$. It is defined as:

$$DM = \frac{d_a + d_b \sum_{i=1}^{|\tilde{\Gamma}|} \left| \hat{d}_i - \bar{d} \right|}{d_a + d_b \left(|\tilde{\Gamma}| - 1 \right) \bar{d}} \tag{40}$$

where $\hat{d}_i$ is the Euclidean distance between two consecutive solutions in $\tilde{\Gamma}$, d_a and d_b are the Euclidean distance between the extreme solutions in $\tilde{\Gamma}$ and Γ respectively.

5.3.5.3 Test instances

To investigate the performance of MCTLBO, five different benchmark test problems namely SCH, KUR, ZDT1, ZDT3 and ZDT6 are considered. The objective functions, variables, variable bounds, and the true Pareto-optimal solutions (D) of those benchmark problems are shown in Table 2.

The tuned values of three parameters of MCTLBO such as number of teachers *nt*, the population size *s* and maximum number of iterations n_i are 3, 100 and 250 respectively. A total of 50 nos. of trial runs have been performed. Results obtained for generational distance and diversity matrix are shown in Table 3 and 4. From Table 4 it is evident that MCTLBO produces best results on the average of generational distance for each benchmark problem. Table 5 shows that MCTLBO generates more uniformly distributed results for all problems except for ZDT3.

Table 2 Benchmark problems

Problem	*Definition (minimisation)*	*Variable bounds*
SCH	$f_1(x) = x^2,\ f_2(x) = (x-2)^2$	$x = [-10^3, 10^3]$
KUR	$f_1(x) = \sum_{i=1}^{D}\left(-10\exp\left(-0.2 * \sqrt{x_i^2 + x_{i+1}^3}\right)\right)$	$x = \in [-5, 5]$
	$f_2(x) = \sum_{i=1}^{D}\left(\lvert x_i\rvert^{0.8} + 5\sin x_i^3\right)$	$D = 3$
ZDT1	$f_1(x) = x_1$	$x_i \in [0, 1]$
	$f_2(x) = g(x)\left[1 - \sqrt{x_1 / g(x)}\right]$	$D = 30$
	$g(x) = 1 + 9\left(\sum_{i=2}^{D} x_i\right) / (D-1)$	
ZDT3	$f_1(x) = x_1$	$x_i \in [0, 1]$
	$f_2(x) = g(x)\left[1 - \sqrt{x_1 / g(x)} - x_1 / g(x)\sin 10\pi x_1\right]$	$D = 30$
	$g(x) = 1 + 9\left(\sum_{i=2}^{D} x_i\right) / (D-1)$	
ZDT6	$f_1(x) = 1 - \exp(-4x_1)\sin^6(6\pi x_1)$	$x_i \in [0, 1]$
	$f_2(x) = g(x)[1 - f_1(x) / g(x)^2]$	$D = 10$
	$g(x) = 1 + 9\left(\sum_{i=2}^{D} x_i\right) / (D-1)$	

Note: D = the number of variable in a problem.

Table 3 Results of generational distance

Problem	*GD*	*NSGA-II*	*MOPSO*	*MCTLBO*
SCH	Average	8.016e-03	1.178e-01	*2.877e-04*
	Standard deviation	4.159e-03	6.209e-01	1.179e-04
KUR	Average	5.856e-01	1.960e-01	*4.733e-03*
	Standard deviation	4.408e-01	4.486e-02	1.783e-03
ZDT1	Average	4.797e-02	3.156e-01	*1.196e-04*
	Standard deviation	4.985e-02	1.379e-01	3.832e-05
ZDT3	Average	4.560e-02	3.308e-01	*3.196e-04*
	Standard deviation	4.538e-02	2.233e-01	2.278e-05
ZDT6	Average	3.322e-01	8.938e-01	*3.541e-05*
	Standard deviation	2.507e-01	8.310e-01	1.545e-06

Note: Comparison with NSGA-Π and MOPSO

Table 4 Results of diversity metric

Problem	*DM*	*NSGA-II*	*MOPSO*	*MCTLBO*
SCH	Average	4.083e-01	1.231	*3.521e-01*
	Standard deviation	3.003e-02	1.486e-01	2.225e-02
KUR	Average	5.861e-01	1.070	*4.429e-01*
	Standard deviation	9.294e-02	7.409e-02	3.122e-02
ZDT1	Average	3.653e-01	9.835e-01	*3.584e-01*
	Standard deviation	4.420e-02	6.828e-02	2.972e-02
ZDT3	Average	*5.823e-01*	8.841e-01	6.607e-01
	Standard deviation	4.523e-02	6.228e-02	2.195e-02
ZDT6	Average	1.061	1.193	*3.433e-01*
	Standard deviation	1.484e-01	1.202e-01	3.565e-02

Note: Comparison with NSGA-II and MOPSO.

5.3.6 Application of MCTLBO to solve the problem

The system data, constraints, number of students or population size, maximum number of iteration, number of design variables or subjects (courses) offered which coincides with the number of RES units to be placed in the RDS and the limits of design variables (number of RES units placement buses, limits of number of PV and limits of number of BESS) are considered for the optimisation problem. The number of teachers implies to the number of objective functions considered simultaneously for the optimisation problem. RES units' placement buses, number of PV and number BESS are positive integers. The placement bus, number of PV and number of BESS of the RES units are randomly generated and normalised between the maximum and minimum operating limits. The procedure for implementing the MCTLBO algorithm to solve the problem is described in the flowchart, shown in Figure 5.

6 Results and discussions

The performance of the proposed multi-objective MCTLBO optimisation technique was tested in RDS for different scenarios and cases. The parameters of MCTLBO used in simulation were number of teachers = 2. The parameters of NSGA-II used in simulation were crossover distribution index (μ_c) = 20, mutation distribution index (μ_m) = 20, crossover probability (ρ_c) = 0.9 and mutation probability $(\rho_m) = \frac{1}{n}$, where n is the number of decision variables. Maximum number of iteration and population size for both optimised methods were 150 and 50 respectively. The proposed algorithm was executed for various combinations of objective functions considering different cases related to scenario-A and scenario-B as follows:

Scenario-A Power loss ($f_{obj,1}$) and voltage offset ($f_{obj,2}$).

Scenario-B Power loss ($f_{obj,1}$) and security margin ($f_{obj,3}$).

The system used was a 69-bus large-scale RDS (Moradi and Abedini, 2012). Power flow calculation was performed using base value 100 MVA and 12.66 kV, with the current carrying capacity of branches 1–9 being 400 A, and that of branches 46–49 and 52–64 being 300 A. The current capacity of the remaining branches including the tie lines was 200 A. The load bus was considered as the location for the RESs. The specifications of the three RESs were same. Moreover, the hourly insolation data for all the load buses was considered to be same. The bus voltage was limited to 0.95–1.05 p.u. The peak hours of the day were considered to be 7 am to 1 pm and 4 pm to 10 pm. The rest of the hours were considered as off-peak hours.

The analysis of the proposed algorithm for allocation of RESs in RDS was carried out for each scenario considering three case studies:

1 Case #0 (base case): without installing RESs.

2 Case #1: installing three RESs without reactive power generation.

3 Case #2: installing three RESs with reactive power generation at 0.86 leading power factor.

Using multi-objective MCTLBO technique the variables (location of RESs, number of PV and number of BESS) for different cases with optimal solutions are given in Tables 5 and 6. Tables 5 and 6 list the results obtained for scenario-A and scenario-B implementing both MCTLBO and NSGA-II respectively. All the values were calculated as an average value for a day. The results demonstrate that the solutions obtained in case #2 are minimum as compared with other cases. The proposed method was simulated for all the cases. From the result, reduction in both power loss and voltage offset for Scenario-A and reduction in power loss with improvement in security margin for Scenario-B considering both the cases has been noted. The proposed method was simulated for two scenarios considering two cases and the distribution of Pareto solutions are shown in Figures 6–7 using multi-objective MCTLBO and NSGA-II. These figures are self-explanatory of the fact that MCTLBO produces better result than NSGA-II.

Figure 6 Pareto front for scenario-A, (a) case #1 (b) case #2 (see online version for colours)

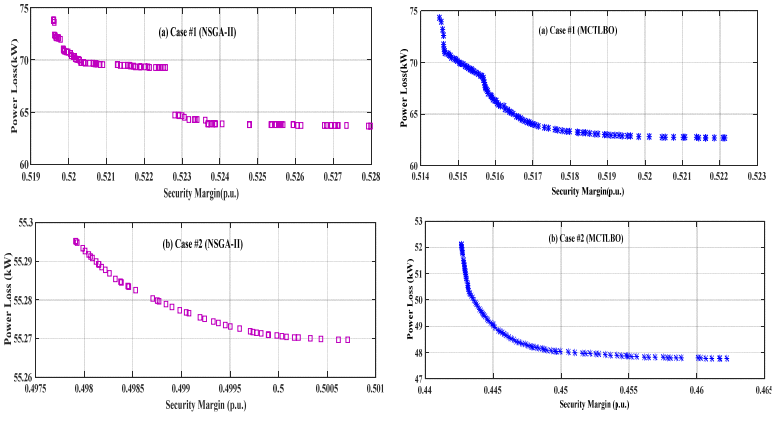

Table 5 Objective function values and solutions for Scenario-A

Parameters	*Base case case #0*	*Case #1*		*Case #2*	
		NSGA-II	*MCTLBO*	*NSGA-II*	*MCTLBO*
Function					
Power loss($f_{obj,1}$)	97.74	65.20	62.99	56.83	47.99
Voltage offs ($f_{obj,2}$)	0.2740	0.2049	0.1914	0.2028	0.1866
Variable					
Location	-				
RES unit 1		59	17	69	61
RES unit 2		62	64	64	64
RES unit 3		61	61	63	15
No. of PV	-				
PV of unit 1		278	350	338	350
PV of unit 2		348	350	330	349
PV of unit 3		252	350	87	350
No. of battery	-				
BESS of unit 1		87	25	28	142
BESS of unit 2		24	4	178	1
BESS of unit 3		138	195	88	7

Figure 7 Pareto front for scenario-B, (a) case #1 (b) case #2 (see online version for colours)

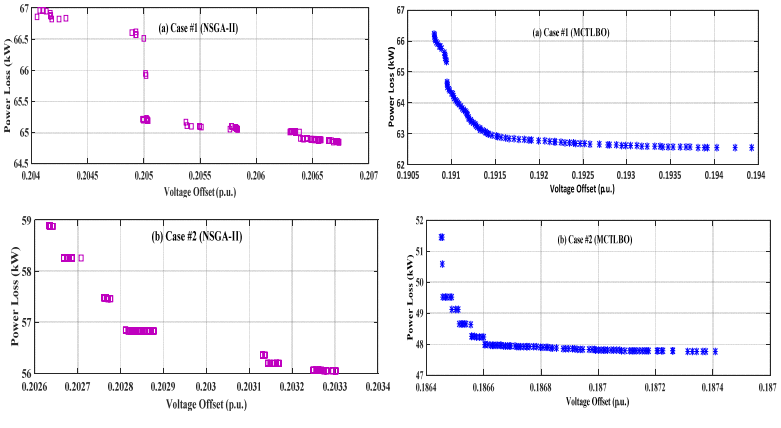

Figure 8 depicts 65-bus voltage profile for two scenarios considering all cases for one day as the voltage level of 65-bus was low compared with that of other buses. Before installation of RESs, the voltage level of bus 65 was low and after installation the voltage profile was improved.

Table 6 Objective function values and solutions for scenario-B

Parameters	*Base case case #0*	*Case #1*		*Case #2*	
		NSGA-II	*MCTLBO*	*NSGA-II*	*MCTLBO*
Function					
Power loss($f_{obj,1}$)	97.74	64.71	64.22	55.27	48.33
Security Margi ($f_{obj,3}$)	0.6319	0.5227	0.5168	0.4990	0.4471
Variable					
Location	-				
RES unit 1		64	61	60	61
RES unit 2		62	62	61	61
RES unit 3		18	12	45	12
No. of PV	-				
PV of unit 1		332	350	261	350
PV of unit 2		326	350	350	350
PV of unit 3		311	350	132	350
No. of battery	-				
BESS of unit 1		103	138	44	77
BESS of unit 2		103	150	176	150
BESS of unit 3		178	200	32	106

Figure 8 Voltage profile of bus 65 for (a) scenario-A and (b) scenario-B (see online version for colours)

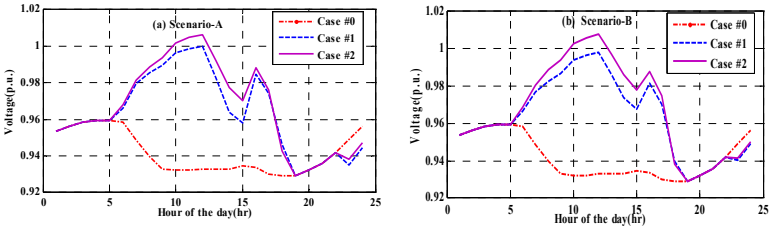

The voltage profile of 69-bus RDS for all buses is shown in Figure 9. It is observed that voltage profile of case #2 is better than others.

Figure 10 shows the power imported from the high voltage (HV) grid at the substation for the base case with and without reactive power injection. A considerable improvement in terms of the levelling power was obtained. As per the operational strategy adopted, the power drawn from the upstream grid was reduced, which was compensated by the proposed RESs during the peak hours. The BESS units were discharged during peak hours and charged during the off-peak hours to alleviate upstream congestion by supplying downstream, transmission–distribution upgrade deferral, demand charge management, renewable energy time shift, and renewable capacity firming.

Figure 9 Voltage profile of 69 bus network for (a) scenario-A and (b) scenario-B (see online version for colours)

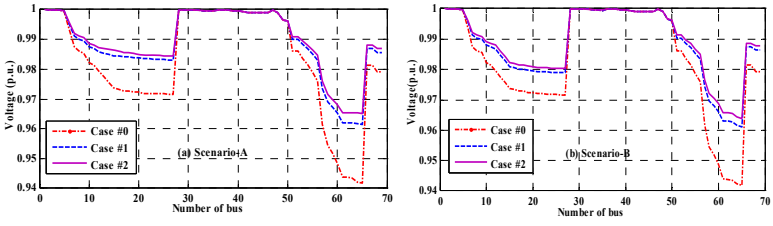

Figure 10 Active power imported from the HV grid, (a) scenario-A (b) scenario-B (see online version for colours)

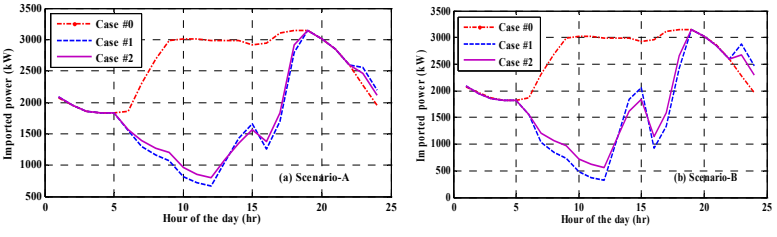

Same type of BESS was used in all RESs. So the SOC curves were same. Figure 11 shows that the BESS remains idle from the start of the day to 7 am as it has maximum charge. After 7 am, as the peak hour starts, the BES discharges to supply the load until 1 pm Then, it charges during the off-peak hour until 4 pm After 4 pm, the BESS starts discharging until 7 pm during the evening peak hour and reaches the minimum SOC of 30%. Then, it remains idle and again starts charging at 11 pm as the off-peak hour starts.

Figure 11 Variation of SOC of BESS at optimal locations (see online version for colours)

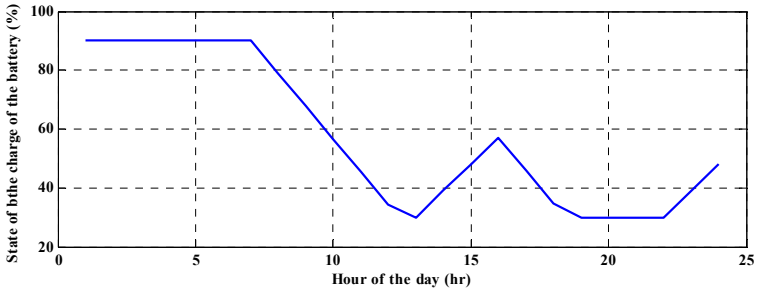

Figures 12–13 show that during the peak period of the day, the BESS supplies power to the grid and charged during off-peak period. During the peak hour, the grid demand is met by the RESs, to maintain the voltage profile of distribution system at its desire level.

Figure 12 Active power variation of PV, grid and BES [scenario-A] for case #2 (see online version for colours)

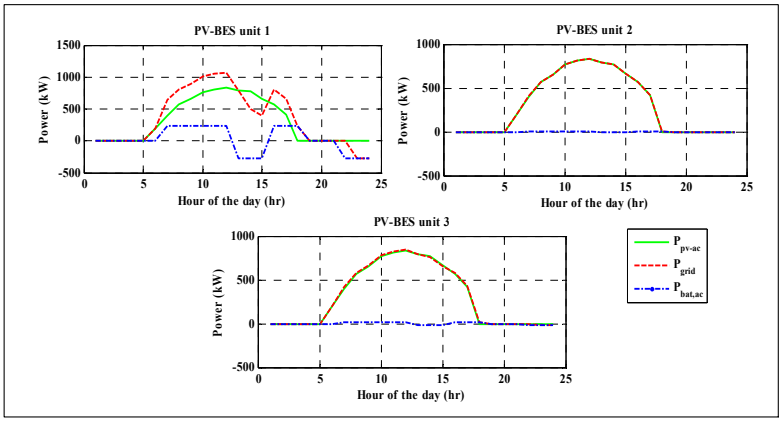

Figure 13 Active power variation of PV, grid and BES [scenario-B] for case #2 (see online version for colours)

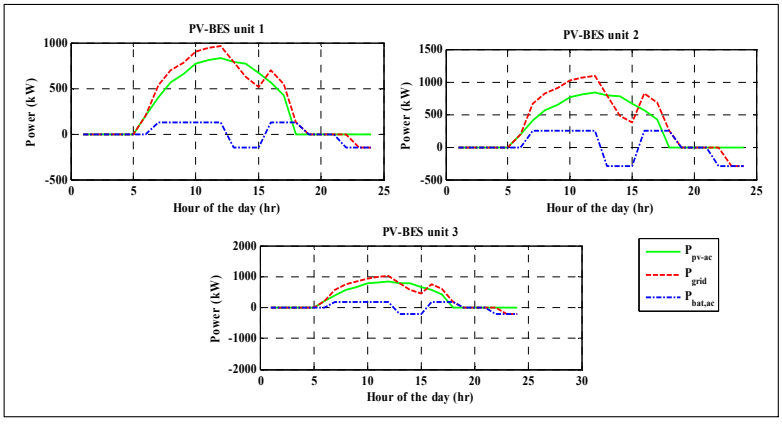

From an annual perspective, the financial benefits of the proposed method are listed in Table 5 based on TOU tariff. The purchase rates of INR 12.20/kWh and INR 5.00/kWh were considered for the peak and off-peak hours, respectively. This table presents the annual savings in energy losses of the system, cost of power loss, cost benefits obtained

from discharging the BESS to the PV-integrated system and cost of the power purchased from HV grid. The table is evident of the fact that the energy loss decreases and cost benefit increases if reactive power is injected into the system for both the scenarios.

Table 7 Techno-economic analysis

Cases	*Energy losses savings (kWh)*	*Cost of power losses in INR*	*Cost benefit of discharging power of BESS in INR*	*Cost of power purchased from HV grid in INR*
Case #0	-	8,690,297	-	223,052,797
Scenario-A				
Case #1	304,449	5,285,936	253,050	219,648,436
Case #2	435,825	3,879,842	294,708	218,242,342
Scenario-B				
Case #1	293,606	5,284,569	337,218	219,647,069
Case #2	432,835	3,817,070	416,688	218,179,570

7 Conclusions

In this study, a new methodology has been presented for integration of renewable energy system (RES) such as photovoltaic/battery energy storage system (PV/BESS) in 69-bus RDS considering two multi-objective problems with and without reactive power injection. A novel multi-objective MCTLBO algorithm has been proposed for allocation of RESs in RDS. Test results showed that if the power flow between RESs and RDS can be done effectively, then the improved performance of RDS can be achieved. The purchase and sell of energy with the grid is done by using TOU tariff in order to get many technoeconomic benefits such as cost, regulation service, voltage support, peak-load shifting and reliability improvement.

References

(1999) 'RTS task force: the IEEE reliability test system-1996', *IEEE Trans. Power Syst.*, Vol. 14, No. 3, pp.1010–1020.

Aksanli, B. and Rosling, T. (2013) 'Optimal battery configuration in a residential home with time of use pricing', *Proceedings of the IEEE Int. Conference on Smart grid Communication.*

Ali, H. and Khan, F.A. (2013) 'Attributed multi-objective comprehensive learning particle swarm optimization for optimal security of networks', *Appl. Soft Comput.*, Vol. 13, No. 9, pp.3903–3921.

Deb, K., Pratap, A., Agarwal, S. and Meyarivan, T. (2002) 'A fast and elitist multi objective genetic algorithm: NSGA-II', *IEEE T. Evolut. Comput.*, Vol. 6, No. 2, pp.182–197.

Ghazvini, M., Abbaspour-Tehrani-Fard, A. and Fotuhi-Firuzabad, M. (2015) 'A particle swarm optimization based approach to achieve optimal design and operation strategy of standalone hybrid energy systems', *Turk. J. Elec. Eng. and Comp. Sci.*, Vol. 23, No. 2, pp.335–353.

Grigg, C., Wong, P., Albrecht , P., Allan, R., Bhavaraju, M., Billinton, R., Chen, Q., Fong, C., Haddad, S., Kuruganty, S., Li, W., Mukerji, R., Patton, D., Rau, N., Reppen, D., Schneider, A., Shahidehpour, M. and Singh, C. (1999) 'RTS task force: the IEEE reliability test system-1996', *IEEE Trans. Power Syst.*, Vol. 14, No. 3, pp.1010–1020.

Hill, C.A., Such, M.C., Dongmei, C., Gonzalez, J., and Grady, W.M. (1996) 'Battery energy storage for enabling integration of distributed solar power generation', *IEEE Trans. Energy Convers.*, Vol. 11, No. 2, pp.367–375.

Hung, D.Q., Mithulananthan, N. and Bansal, R.C. (2014) 'Integration of PV and BES units in commercial distribution systems considering energy loss and voltage stability', *Applied Energy*, Vol. 113, No. 2, pp.1162–1170.

IEEE Std. (2003) *IEEE Standard for Interconnecting Distributed Resources with Electric Power Systems 1547*, The Institute of Electrical and Electronics Engineers, Inc., 3 Park Avenue, New York, NY 10016-5997, USA.

Kanzumba, K. (2015) 'Optimal scheduled power flow for distributed photovoltaic/wind/diesel Generators with battery storage system', *IET Renewable Power Generation*, Vol. 9, No. 8, pp.916–924.

Kayal, P. and Chanda, C.K. (2013) 'Placement of wind and solar based DGs in distribution system for power loss minimization and voltage stability improvement', *Int. J. Electr. Power Energy Syst.*, Vol. 53, No. 10, pp.795–809.

Khatod, D.K., Pant, V. and Sharma, J. (2013) 'Evolutionary programming based optimal placement of renewable distributed generation', *IEEE Trans Power Syst*., Vol. 28, No. 2, pp.683–695.

Mohammadi, S., Mozafari, B. and Solimani, S. (2014) 'Optimal operation management of microgrids using the point estimate method and firefly algorithm while considering uncertainty', *Turk J. Elec. Eng. and Comp Sci.*, Vol. 22, No. 3, pp.735–753.

Moradi, M.H.,and Abedini, M.A. (2012) 'Combination of genetic algorithm and particle swarm optimization for optimal DG location and sizing in distribution systems', *Int. J. Electr. Power Energy Syst.*, Vol. 34, No. 1, pp.66–74.

Nayak, M.R. and Nayak, C.K. (2013) 'Distributed generation optimal placement and sizing to enhance power distribution network performance using MTLBO', *International Review of Electrical Engineering*, Vol. 6, No. 8, pp.1857–1869.

Omran,W.A., Kazerani, M. and Salama, M.M.A. (2011) 'Investigation of methods for reduction of power fluctuations generated from large grid-connected photovoltaic systems', *IEEE T. Energy Convers.*, Vol. 26, No. 1, pp.318–327.

Rao, R., Savsani, V. and Vakharia, D. (2011) 'Teaching-learning-based optimization: a novel method for constrained mechanical design optimization problems', *Computer-Aided Design*, Vol. 43, No. 3, pp.303–315.

Shanyi, X., Ruicong, Z., Xianhu, L., Baoguo, L., Kai, L. and Qian, A. (2016) 'Self-adaptive genetic algorithm and fuzzy decision based multi-objective optimization in microgrid with DGs', *The Open Electrical and Electronic Engg. J.*, Vol. 10, No 1, pp.46–57.

Sherwood, L. (2011) *US Solar Market Trends, 2010*, Integrated Renewable Energy Council (IREC), P.O. Box 1156, Latham, New York, NY 518-621-7379, USA.

Suchitra, D., Jegatheesan, R. and Deepika, T.J. (2016) 'Optimal design of hybrid power generation system and its integration in the distribution network', *Electrical Power and Energy Systems*, Vol. 82, No. 9, pp.135–149.

Sugihara, H., Yokoyama, K., Saeki, O., Tsuji, K. and Funaki, T. (2013) 'Economic and efficient voltage management using customer-owned energy storage systems in a distribution network with high penetration of photovoltaic systems', *IEEE Trans. Power Syst.*, Vol. 28, No. 1, pp.102–111.

Ton, D., Peek, G.H., Hanley, C. and Boyes, J. (2008) *Solar Energy Grid Integration Systems – Energy Storage (SEGIS-GS)*, Sandia National Laboratories, Albuquerque, New Mexico 87185 and Livermore, California 94550.

Van Veldhuizen, D.A. and Lamont, G.B. (1998) 'Evolutionary computation and convergence to a Pareto front', in *Late Breaking Papers at the Genetic Programming 1998 Conference*, pp.221–228.